

PAPER • OPEN ACCESS

Hybrid graphene-manganite thin film structure for magnetoresistive sensor application

To cite this article: Rasuole Lukose *et al* 2019 *Nanotechnology* **30** 355503

View the [article online](#) for updates and enhancements.





IOP | ebooks™

Bringing you innovative digital publishing with leading voices to create your essential collection of books in STEM research.

Start exploring the collection - download the first chapter of every title for free.

Hybrid graphene-manganite thin film structure for magnetoresistive sensor application

Rasuole Lukose¹ , Nerija Zurauskiene^{1,2} , Saulius Balevicius^{1,2},
Voitech Stankevicius^{1,2}, Skirmantas Keršulis¹, Valentina Plausinaitiene^{1,3} and
Romualdas Navickas²

¹ Department of Material Science and Electrical Engineering, Center for Physical Sciences and Technology, Vilnius, Lithuania

² Faculty of Electronics, Vilnius Gediminas Technical University, Vilnius, Lithuania

³ Institute of Chemistry, Faculty of Chemistry and Geosciences, Vilnius University, Vilnius, Lithuania

E-mail: nerija.zurauskiene@fmnc.lt

Received 26 January 2019, revised 13 April 2019

Accepted for publication 8 May 2019

Published 11 June 2019



CrossMark

Abstract

An increasing demand of magnetic field sensors with high sensitivity at room temperatures and spatial resolution at micro-nanoscales has resulted in numerous investigations of physical phenomena in advanced materials, and fabrication of novel magnetoresistive devices. In this study the novel magnetic field sensor based on combination of a single layer graphene (SLG) and thin nanostructured manganite $\text{La}_{0.8}\text{Sr}_{0.2}\text{MnO}_3$ (LSMO) film—hybrid graphene-manganite (GM) structure, is proposed and fabricated. The hybrid GM structure employs the properties of two materials—SLG and LSMO—on the nanoscale level and results in the enhanced sensitivity to magnetic field of the hybrid sensor on the macroscopic level. Such result is achieved by designing the hybrid GM sensor in a Wheatstone half-bridge which enables to employ in the device operation two effects of nanomaterials—large Lorentz force induced positive magnetoresistance of graphene and colossal negative magnetoresistance of nanostructured manganite film, and significantly increase the sensitivity S of the hybrid GM sensor in comparison with the individual SLG and LSMO sensors: $S = 5.5 \text{ mV T}^{-1}$ for SLG, 14.5 mV T^{-1} for LSMO and 20 mV T^{-1} for hybrid GM at 0.5 T, when supply voltage was 1.249 V. The hybrid GM sensor operates in the range of (0.1–2.3) T and has lower sensitivity to temperature variations in comparison to the manganite sensor. Moreover, it can be applied for position sensing. The ability to control sensor's characteristics by changing technological conditions of the fabrication of hybrid structure and tuning the nanostructure properties of manganite film is discussed.

Keywords: graphene, manganite thin films, nanostructures, magnetoresistance, magnetic field sensors

(Some figures may appear in colour only in the online journal)

1. Introduction

The detection of magnetic fields with increased spatial resolution to micro-nanoscales is very important for magnetometry, magnetic storage, biosensing and other applications [1–5]. Moreover, the increasing use of smart devices with



Original content from this work may be used under the terms of the [Creative Commons Attribution 3.0 licence](https://creativecommons.org/licenses/by/3.0/). Any further distribution of this work must maintain attribution to the author(s) and the title of the work, journal citation and DOI.

incorporated chip-based sensors are becoming very promising for growing automotive and Internet of things industries and Intelligent transport [6–8]. It is of great interest to have low-dimension sensors with increased sensitivity and extended capabilities operating at room temperatures. The discovery of Hall effect in semiconductors and magnetoresistive effects (anisotropic AMR, tunneling TMR, giant GMR and colossal CMR) in magnetic structures encouraged fundamental research [9–11] leading to a number of laboratory-scale and commercially available devices [12–14]. However, each application has its specific requirements for sensitivity, temperature and magnetic field ranges of operation, accuracy, etc. Therefore, the choice of material with special properties and design of sensing element becomes very important.

Recently, it has been demonstrated that nanostructured (polycrystalline with nanosize grains) lanthanum manganite films can be used for the development of magnetic field sensors operating in wide range of temperatures (4–320 K) and magnetic fields (from mT up to megagauss) [15–17]. Manganite films reveal paramagnetic-ferromagnetic phase transition at a *Curie* temperature and exhibit negative colossal magnetoresistance phenomenon which in simplified theoretical explanation is related to the double-exchange mechanism leading to the increase of material conductivity when magnetic moments of manganese ions are aligned in an external magnetic field [18]. Many research groups are interested in so-called extrinsic magnetoresistance [19] phenomena related to spin-polarized tunneling transport across grain boundaries in polycrystalline manganites, since these promise large magnetoresistance values in low magnetic fields [20, 21]. Magnetoresistive sensors based on nanostructured manganite films have large sensitivity [22, 23] in a wide range of temperatures, however, it decreases with increase of temperature in a paramagnetic state and with increase of magnetic field due to magnetoresistance saturation. The other advantage of nanostructured manganite films—they are relatively insensitive to magnetic field direction at high fields, what makes it possible to design so-called B-scalar sensors [14, 24, 25].

One of the most recently studied materials for the development of magnetoresistive sensors is graphene [26], which is a two-dimensional Dirac semimetal with a very high mobility of charge carriers. The operation of graphene sensor is based on Lorentz force induced positive magnetoresistance phenomenon (Gauss effect). It was shown [27] that such sensors are 100 times more sensitive to magnetic field than silicon equivalent and graphene magnetoresistance does not saturate up to very high fields (62 T) [28]. Graphene sensor can achieve very large magnetoresistance values at intermediate and high magnetic fields (5–15 T) [29–32], however, at low fields (<1 T) the sensitivity of such sensors is low due to classical quadratic MR dependence on magnetic flux density B [33]. Thus low sensitivity of graphene based magnetic field sensor in the low field range up to few tesla and saturation of the sensitivity of manganite based sensor at high magnetic fields are the main disadvantages of these devices. Moreover, the zero magnetic field resistivity of both manganite film and graphene layer at temperatures around

room temperature decreases with increase of temperature (semiconducting state), what makes the sensor's response sensitive to the ambient temperature variations.

In this paper, we suggest the magnetic field sensor based on combination of graphene layer and thin nanostructured manganite film—hybrid graphene-manganite (GM) sensor, which in comparison to an individual graphene or manganite sensors, has significantly larger sensitivity to magnetic field and lower sensitivity to ambient temperature variations.

2. Experimental

2.1. Graphene sensing element fabrication

The commercially available single layer graphene (SLG) grown on Cu foil by chemical vapor deposition method and covered with Poly(methyl methacrylate) (PMMA) polymer was used in the present investigations. The graphene grown on Cu foil was transferred to target substrate Si/SiO₂–100 nm with already formed Ag contacts by applying wet chemical etching procedure. Firstly, Cu foil was chemically dissolved from the bottom of Cu/Graphene/PMMA structure and, as a result, the SLG + PMMA flake was floating on the top of etching solution surface. Afterwards rinsing with deionized water was performed and the floating flake was 'caught' and transferred on the top of target substrate with already formed Ag contacts. The PMMA layer was left as the protection of graphene layer in order to prevent additional oxygen contamination and altering of electric and magnetic properties of graphene during the time.

2.2. Nanostructured manganite film fabrication

The La_{1-x}Sr_xMnO₃ (LSMO) films with a thickness of 350 nm were deposited using a pulsed-injection metal-organic chemical vapor deposition technique [34] onto a polycrystalline Al₂O₃ substrate. Such substrate was chosen in order to grow nanostructured films with nanosize crystallites. After flash evaporation (at ~270 °C) of the micro-doses, the resulting vapor mixture was transported by an Ar + O₂ (3:1) gas flow towards the heated substrate. During the growth, the temperature of the substrate was kept at 750 °C and injection frequency was 2 Hz. A total pressure of Ar + O₂ gases in reactor was 10 Torr.

2.3. Morphology and microstructure characterization

The surface morphology and microstructure of the LSMO film was investigated by scanning electron microscope (SEM) and transmission electron microscope (TEM). The Sr content x in the grown films was estimated by energy-dispersive x-ray spectroscopy measurements and was found almost constant: $x = 0.2 \pm 0.01$.

2.4. Electrical transport and magnetoresistance measurements

The dependence of manganite film and graphene layer resistances on temperature was investigated in the range from 5 to 320 K using closed cycle helium cryo-cooler (JANIS). The magnetoresistance of individual graphene or manganite sensors as well as hybrid sensor's response to magnetic field was investigated using electromagnet which was able to generate DC magnetic field up to 2.35 T. The response to magnetic field from hybrid graphene-manganite sensor was recorded by measuring the change of voltage drop ΔV_{res} across the manganite film, when the circuit was supplied by source voltage of $V_S = 1.249$ V. The investigation of the sensor's response to magnetic field direction was performed by rotation of the electromagnet.

3. Results and discussion

3.1. Design of hybrid GM structure

The proof-of-concept of the proposed GM magnetic field sensor is realized by fabrication of a hybrid structure composed of a SLG and nanostructured manganite $\text{La}_{0.8}\text{Sr}_{0.2}\text{MnO}_3$ (LSMO) film (see figure 1). The surface morphology and microstructure of the hybrid GM structure is presented in figures 1(a)–(c). SEM images of graphene layer covered by Poly(methyl methacrylate) (PMMA) polymer and manganite film with electrodes (1, 2, 3) are shown in figures 1(a), (b), respectively. In the first image (a) we can see only the surface of PMMA covering the graphene layer, while in the second image (b) the surface of the manganite film (LSMO) between two electrodes (2 and 3) is clearly observed. Additionally, figure 1(c) shows the enlarged view of the manganite film surface (upper SEM image) and cross section of the film obtained by TEM presented in the lower image. One can see that the 350 nm thick film is nanostructured with well-pronounced crystalline columns spread throughout the entire thickness of the film in the direction perpendicular to the substrate plane. The crystallite columns having width of 50–70 nm were separated by 5–7 nm thick vitreous grain boundaries (evaluated from high-resolution TEM).

The hybrid GM sensor was designed as a Wheatstone half-bridge (voltage divider, see figure 1(d)) with three terminal (1, 2, 3) electrical circuit which consisted of a power supply of voltage V_s and two magnetic field sensing elements connected in series: SLG (4) and nanostructured manganite film LSMO (5) represented in the figure 1(d) as resistors R_{SLG} and R_{LSMO} , respectively. The response voltage V_{res} in applied magnetic field was measured across the manganite film. An increase of sensitivity of the proposed device was expected as a result of opposite signs of magnetoresistance phenomena in graphene and manganite film. The schematic structure of both sensing elements SLG and LSMO is shown in figures 1(e), (f).

For the proof-of-concept, two designs of hybrid GM sensor were proposed and investigated: coplanar and

perpendicular (see figure 1(g), (h)). In case of coplanar design (g), the graphene layer and manganite film were placed and connected in the same plane. In this case the applied magnetic field was directed with the same angle in respect to the plane of both sensing elements. For the perpendicular design (h), the manganite film plane was perpendicular to the graphene layer plane. In such case the magnetic field applied perpendicular to the graphene layer was directed parallel to the manganite film plane.

It has to be noted, that magnetoresistive properties of individual sensors, fabricated only from single graphene layer (figure 1(e)) or manganite film (figure 1(f)), were also investigated. In this case, the graphene layer or manganite film was connected in a voltage divider circuit connecting them in series with a ballast resistor replacing R_{LSMO} or R_{SLG} , respectively, in the circuit presented in figure 1(d). The value of resistance of the ballast resistor was chosen the same as that of graphene or manganite film in order to ensure the same conditions as for the hybrid GM sensor in zero magnetic field.

3.2. Magnetoresistance and sensitivity of the hybrid GM sensor

Figure 2 presents the magnetoresistance (MR) of SLG and nanostructured manganite film (LSMO) defined as follows:

$$\text{MR} = \frac{\Delta R}{R(0)} \cdot 100\% = \frac{R(B) - R(0)}{R(0)} \cdot 100\%, \quad (1)$$

where $R(B)$ and $R(0)$ are resistance values at magnetic field B and zero field, respectively. One can see that the graphene layer exhibits positive while nanostructured manganite film negative magnetoresistance phenomena. In order to compare the influence of magnetoresistive properties of individual sensors based on SGL or LSMO films on the sensitivity of the hybrid structure, the SLG was chosen with similar MR values as LSMO film in the investigated magnetic field range. One can see that at low field ($B < 1.5$ T) the MR dependence is quadratic and thus the SLG sensor has low sensitivity to magnetic field in this range. At higher fields ($B > 1.5$ T) the MR behavior changes to linear [28, 29] and the slope of this dependence is very important for the sensitivity of magnetic field sensor. Also, it has to be pointed out that the MR of SLG is maximal when B is perpendicular to the layer plane and zero if it is applied in the plane, what is typical for Lorentz force magnetic field sensors. In contrary, the value of MR of manganite film only slightly depends on the direction of magnetic field (MR anisotropy $\text{MRA} = (\text{MR}_{||} - \text{MR}_{\perp})/\text{MR}_{||}$) in respect to the film plane (B parallel $||$ or perpendicular \perp). The MRA significantly decreases with increase of magnetic field and at 2 T is of the order of 10% (in the field higher than 10 T it is less than 2%). Such behavior of the MR is a result of a special nanostructure of manganite film. Due to demagnetization (shape) effect related with aspect ratio of thin film geometry, the direction of easy-axis of magnetization is aligned with the film plane [35–37]. In our case of nanostructured LSMO film, such effect is partly compensated by column-like crystallite structure, in which the easy-axis of magnetization in a single columnar crystallite is directed along its axis perpendicular to

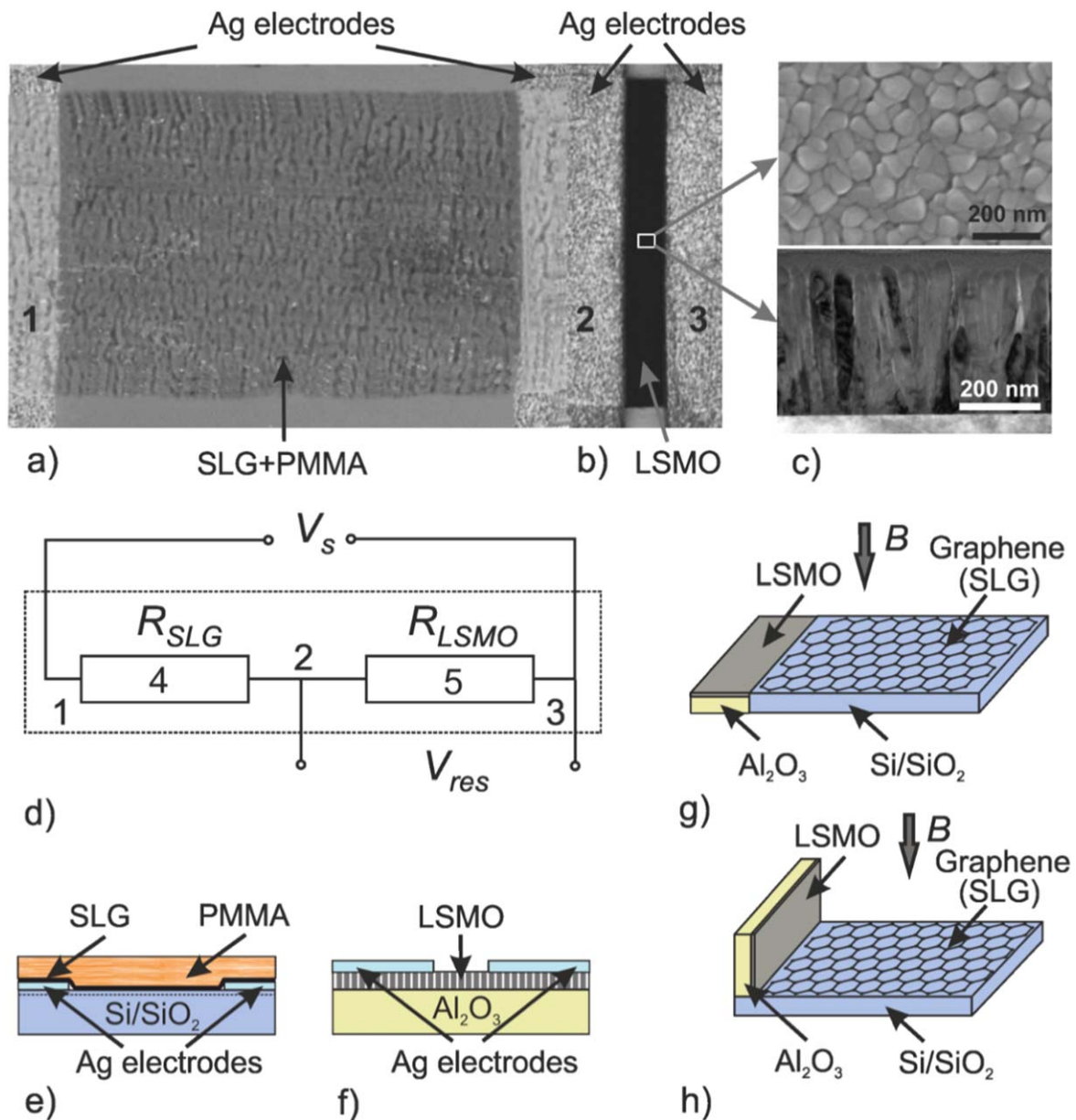


Figure 1. SEM images of graphene (SLG) covered with PMMA (a) and nanostructured manganite film. (b) 1, 2 and 3 are Ag electrodes. (c) Enlarged part of manganite film surface (upper image obtained by SEM) and cross section view (lower image obtained by TEM). (d) Electrical circuit of hybrid graphene-manganite (GM) sensor. (e) Schematic diagram of graphene sensor consisting of SLG covered with PMMA and transferred on Si/SiO₂ substrate with formed in advance Ag electrodes. (f) Schematic diagram of manganite sensor consisting of nanostructured manganite film deposited on Al₂O₃ substrate and Ag electrodes. (g) Coplanar GM sensor's design. (h) Perpendicular GM sensor's design.

the film plane. Moreover, depending on thickness of crystalline columns and properties of grain boundaries with reduced magnetization and crystalline order [38], it is possible to tune the magnetoresistance magnitude of the nanostructured films [34] and change compensation level of the demagnetization field [23, 37]. As a result, the magnetoresistance anisotropy can be minimized [23, 34]. It has to be noted that figure 2 presents only one case—the results of the La_{0.8}Sr_{0.2}MnO₃ film which nanostructure is presented in figure 1(c). Changing film's nanostructure by technological conditions [34] and the aspect ratio of the film geometric

shape (decreasing planar dimensions down to film thickness) it is possible to minimize the demagnetization field and thus to achieve similar MR values for both perpendicular and parallel field directions.

Two effects of nanomaterials—large positive magnetoresistance of graphene at high (>1 T) magnetic fields [28–31] and large negative magnetoresistance of nanostructured strontium manganite films [17] at room temperature from low fields up to intermediate fields—allowed us to propose hybrid graphene-manganite sensor expecting to increase the sensitivity to magnetic field in a wide magnetic field range.

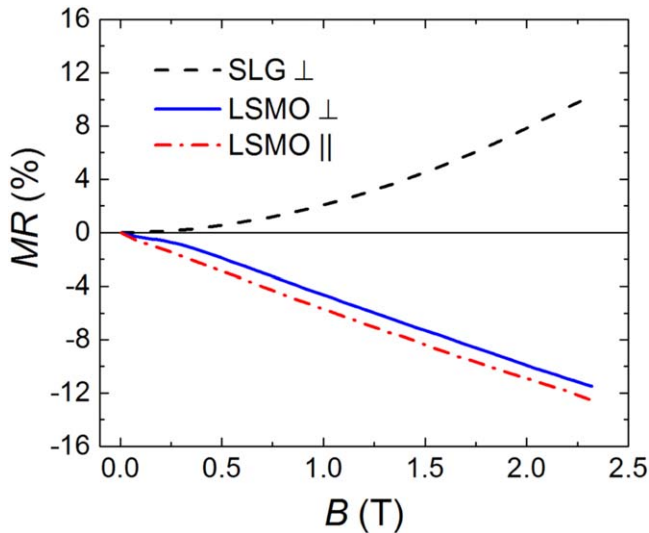


Figure 2. Magnetoresistance (MR) of graphene layer (dashed black curve) and manganite film at two different orientations of magnetic field at room temperature ($T = 294$ K). Dashed–dotted red curve obtained when B was parallel to the film plane, the solid blue curve was measured when B was perpendicular to this plane.

Figure 3 a presents the results of the absolute value of response voltage change $\Delta V_{\text{res}} = |V_{\text{res}}(B) - V_{\text{res}}(0)|$ with magnetic field B for hybrid GM sensor measured using electrical circuit presented in figure 1(d) at two configurations of magnetic field: when B is aligned perpendicular to graphene layer and parallel (solid red line, upper graph) or perpendicular (solid blue line, lower graph) to manganite film plane. The dependences of ΔV_{res} versus B for individual sensors made only from graphene layer (black dashed curves) or manganite film (dash–dot curves) are also presented for the comparison. One can see that the voltage response from the hybrid GM sensor is larger in comparison with response from individual sensors. The most significant increase of the hybrid GM response is observed at low fields (<1.5 T), where ΔV_{res} from the individual SLG sensor is very small. Such effect is a result of change of the fraction of voltage drop across one element (manganite) due to change of the resistance of another element (graphene) because of different signs of magnetoresistance of both elements.

The absolute sensitivity of the sensors to magnetic field was defined as $S = \delta\Delta V_{\text{res}}/\delta B$. The dependences of S versus B for two GM sensor configurations obtained from data presented in figure 3(a) are shown in figure 3(b). One can see, that in the range of (0–1.5) T the sensitivity of individual LSMO is higher in comparison to the individual SLG sensor. At higher fields, the sensitivity of the SLG sensor becomes higher. As a result, the total sensitivity of the hybrid GM sensor is always higher in the measured magnetic field range in comparison to the individual LSMO or SLG sensors. Figure 3(b) shows that at low magnetic field the sensitivity of manganite film is significantly higher if magnetic field is oriented along the film plane (perpendicular configuration). Due to demagnetization (shape) effect in thin manganite film, the S versus B dependence (lower graph in figure 3(b)) consists of two regions with different slopes demonstrating

different nonlinearity of ΔV_{res} versus B characteristic. Thus the design in which graphene layer and manganite film planes are perpendicular each to the other is preferable for magnetic field sensor as in this case the nonlinearity of ΔV_{res} versus B characteristic in all measured magnetic field range is described by one and the same law ($\Delta V_{\text{res}} \sim B^2$). This also makes less complicated calibration procedure of the sensor in comparison to the coplanar case. It has to be noted, that for sensor applications the constant sensitivity is preferable. However, it usually can be achieved only in narrow magnetic field range $(\Delta B)_{\text{linear}}$. For example, GMR or TMR sensors have linear response and constant sensitivity in mT range [39]. In such case the sensitivity is defined as $\text{MR}/(\Delta B)_{\text{linear}}$ which can be increased several times by decreasing the saturation field and measurement range. In the case of graphene, the linear response can be achieved at much wider range up to very high magnetic fields (from 1 T up to 62 T at room temperature [28]). However, at lower fields the MR has B^2 dependence [28, 29]. Therefore, for sensors applications in a wide magnetic field range, nonlinear characteristics are not a problem: one can use modern electronics and signal conditioning circuits with stored in advance calibration data [14]. In our proposed device the magnetoresistance change of graphene and manganite elements has different signs, thus we evaluated the sensitivity of the hybrid GM structure and compared it with the sensitivities of individual elements as response voltage change relative to the magnetic field change. For comparison, the S value in hybrid GM sensor of perpendicular configuration in respect to the individual graphene layer sensor increases approximately 13 times at $B = 0.1$ T and 4 times at $B = 0.5$ T (figure 3(b), upper graph). However, when both graphene and manganite planes are in parallel, the S value changes from 7 to 3.7 times (figure 3(b), lower graph), respectively. This demonstrates that sensor in which graphene and manganite planes are perpendicular each to the other exhibits larger sensitivity in comparison to coplanar design. However, if the nanostructure of LSMO film and the aspect ratio of its geometric shape was optimized, it would be possible to minimize the demagnetization field and to achieve high sensitivity of the hybrid GM sensor at low magnetic fields using more technologically convenient coplanar configuration: $\text{LSMO}\perp + \text{SGL}\perp$, when both layers are in one plane.

It is important to note that the sensitivity S of the GM sensor also depends on the supply voltage V_s of the measurement circuit (see figure 1(d)). Therefore, in the general case we have to consider a relative voltage change of the sensor's response in respect to the supply voltage: $\Delta V_{\text{res}}/V_s$. For example, at 0.5 T the voltage normalized sensitivity $S_V = S/V_s$ when $V_s = 1.249$ V is the following: 0.0044 V/VT, 0.0116 V/VT, and 0.016 V/VT for individual SLG, LSMO and hybrid GM sensors. In comparison, the Hall sensor based on silicon achieved $S_V = 0.1$ V/VT, based on graphene (0.35–3)V/VT (see, for example, a comparison table in [40]), however, these sensors were operating only in mT range. It is obvious that the maximal sensitivity of the hybrid GM sensor depends on the intrinsic properties of both manganite film and graphene layer in magnetic field

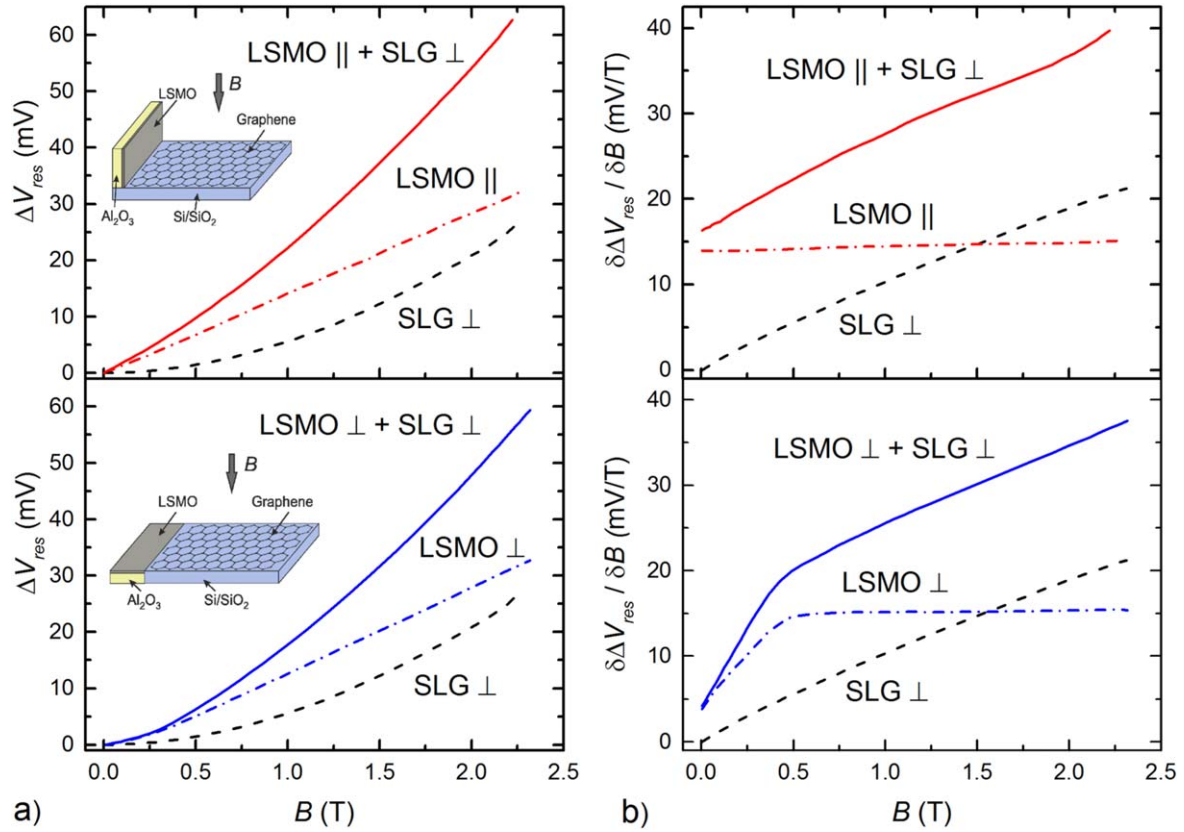


Figure 3. (a) The voltage response change ΔV_{res} dependence on magnetic flux density B for hybrid GM sensor, when magnetic field is applied perpendicular to graphene layer and parallel to manganite film (upper graph, solid red line) or perpendicular to both graphene and manganite planes (lower graph, solid blue line). The dashed black curve represents voltage response change from individual graphene sensor ($\text{SLG} \perp$), while dashed–dotted lines represent voltage response from individual manganite sensor when magnetic field was applied parallel ($\text{LSMO} \parallel$) or perpendicular ($\text{LSMO} \perp$) to the film plane. (b) The sensitivity S of different sensors obtained from corresponding curves presented in graph (a). Power supply voltage $V_s = 1.249$ V, ambient temperature $T = 294$ K.

(magnetoresistance dependences on B , see figure 2) as well as on the resistance values of both elements in zero magnetic field. Therefore, we expressed the relative voltage change in a form of its dependence on the absolute values of magnetoresistances MR_{SLG} and MR_{LSMO} as well as resistances $R_{\text{SLG}}(0)$ and $R_{\text{LSMO}}(0)$ of the SLG and manganite LSMO, respectively.

According to the electrical circuit shown in figure 1(d), the hybrid GM sensor's response change is the following:

$$\Delta V_{\text{res}} = V_s \cdot \left[\frac{R_{\text{LSMO}}(B)}{R_{\text{LSMO}}(B) + R_{\text{SLG}}(B)} - \frac{R_{\text{LSMO}}(0)}{R_{\text{LSMO}}(0) + R_{\text{SLG}}(0)} \right]. \quad (2)$$

It could be expressed in the form:

$$\frac{\Delta V_{\text{res}}}{V_s} = \frac{1}{1 + r \cdot m} - \frac{1}{1 + r}. \quad (3)$$

Here the following parameters r and m are introduced:

$$r = \frac{R_{\text{SLG}}(0)}{R_{\text{LSMO}}(0)}; \quad (4)$$

$$m = \frac{1 + |\text{MR}_{\text{SLG}}|}{1 - |\text{MR}_{\text{LSMO}}|}; \quad (5)$$

$$\text{MR}_{\text{SLG}} = \frac{R_{\text{SLG}}(B)}{R_{\text{SLG}}(0)} - 1;$$

$$\text{MR}_{\text{LSMO}} = \frac{R_{\text{LSMO}}(B)}{R_{\text{LSMO}}(0)} - 1. \quad (6)$$

It has to be noted, that the MR_{SLG} and MR_{LSMO} in equation (6) are measured not in percentage (as MR in equation (1) and figure 2), but in parts of the unit (MR/100%). It was shown (see figure 2) that the magnetoresistance of graphene is positive, while manganite exhibits negative MR, for this reason the sign in front of the absolute value of the MR_{LSMO} in equation (5) is negative.

Equation (3) can be used to determine the required parameters of LSMO and SLG in order to obtain maximal relative response of the hybrid GM sensor. For example, zero

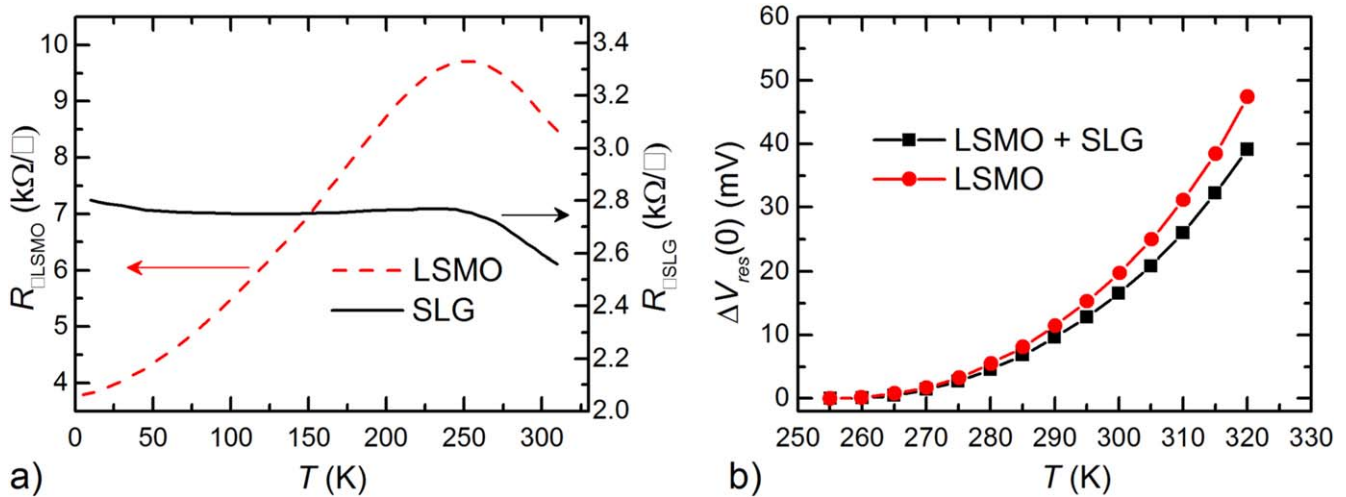


Figure 4. (a) Sheet resistance versus temperature dependences for single layer graphene SLG (black solid curve) and thin manganite film LSMO (red dashed curve). (b) The absolute value of voltage response change $\Delta V_{\text{res}}(0)$ with temperature in the temperature range of (250–320) K in zero magnetic field for hybrid GM sensor (circular red dots) and sensor based only on manganite film (black square symbols).

field resistances of our fabricated individual LSMO and SLG sensors were 670Ω and 283Ω , respectively, while the magnetoresistance magnitudes at 2 T were 11% and 7.9%, respectively (see figure 2). Therefore, from equations (4), (5) we obtain the following values of parameters: $m = 1.21$, $r = 0.42$, and from equation (3) the absolute value of relative response $\Delta V_{\text{res}}/V_s = 0.04$. When $V_s = 1.249 \text{ V}$, using equation (3) we determine $\Delta V_{\text{res}} = 0.051 \text{ V}$, what is in agreement with the measured value $\approx 52 \text{ mV}$ (see figure 3(a)). From the equation (3) follows, that the maximal sensitivity of the hybrid GM sensor in the investigated magnetic field range can be obtained when the resistances of SLG and LSMO film are of similar value. Moreover, the relative response can be increased by increasing the parameter m —increasing the MR of graphene and manganite by optimizing fabrication technology of both layers. For example, if MR of LSMO would be increased up to 16% at 2 T by using two sources of precursors supply during PI MOCVD technology proposed in [41] and the MR of graphene would be increased up to 100% using optimized graphene preparation technology on BN substrate (see [42]), the parameter $m = 2.38$. Keeping the same ratio of zero field resistances $r = 0.42$ and $V_s = 1.249 \text{ V}$, one can calculate response $\Delta V_{\text{res}} = 0.250 \text{ V}$, which is increased by 5 times in comparison with our presented case.

3.3. Temperature dependence

Very important parameter of magnetic field sensor is zero field resistance sensitivity to temperature variations. Figure 4 demonstrates sheet resistance (R_{\square}) dependence on temperature (T) for graphene layer (SLG) and thin manganite film (LSMO). The metal–insulator transition temperature which corresponds to the temperature of resistivity maximum (T_m) of LSMO film is 250 K.

As it can be seen, in temperature range from 275 K to 320 K both graphene and manganite exhibits semiconductor-type R_{\square} versus T behavior with $-24 \Omega/\text{K}$ and $-4 \Omega/\text{K}$

resistance temperature coefficient (RTC), respectively. This means that the most sensitive to temperature variations element of the hybrid graphene-manganite sensor is manganite film. However, when two active elements (LSMO and SLG) are connected into a hybrid GM sensor, the voltage response change due to change of ambient temperature is less pronounced. Figure 4(b) shows the absolute value of zero field voltage response change $\Delta V_{\text{res}}(0) = V_{\text{res}320\text{K}}(0) - V_{\text{res}250\text{K}}(0)$ versus temperature in the semiconducting state (250–320 K) for the sensor consisting of individual manganite film (red circular dots) and the hybrid graphene-manganite sensor (black squares). As it can be seen, in the temperature range from 290 to 320 K the voltage response change is about 17% less for hybrid GM sensor in comparison with the LSMO sensor. The sensitivity to temperature variations can be significantly decreased by using manganite film with lower RTC value. The technological method to decrease RTC value for manganite films was proposed by co-authors in EU patent [43] connecting two LSMO films with different metal–insulator transition temperature values. Moreover, the calibration data of the sensor prepared in advance in the whole operation range of temperature and magnetic field could be stored in modern electronics module and used during measurements to convert measured response voltage change to magnetic flux values [14].

3.4. Application for position sensing

The hybrid graphene-manganite sensor is a composition of two sensors: one is Lorentz force sensor which signal strongly depends on direction of magnetic field (it is zero if B is parallel to the graphene plane) and CMR-B-scalar sensor having small sensitivity to the orientation of magnetic field. This makes it possible to use the hybrid GM sensor also as a position sensor for various applications [44–46]. Figure 5(a) shows the response from the GM sensor at two magnetic field orientations: (1) when B is parallel to both graphene and

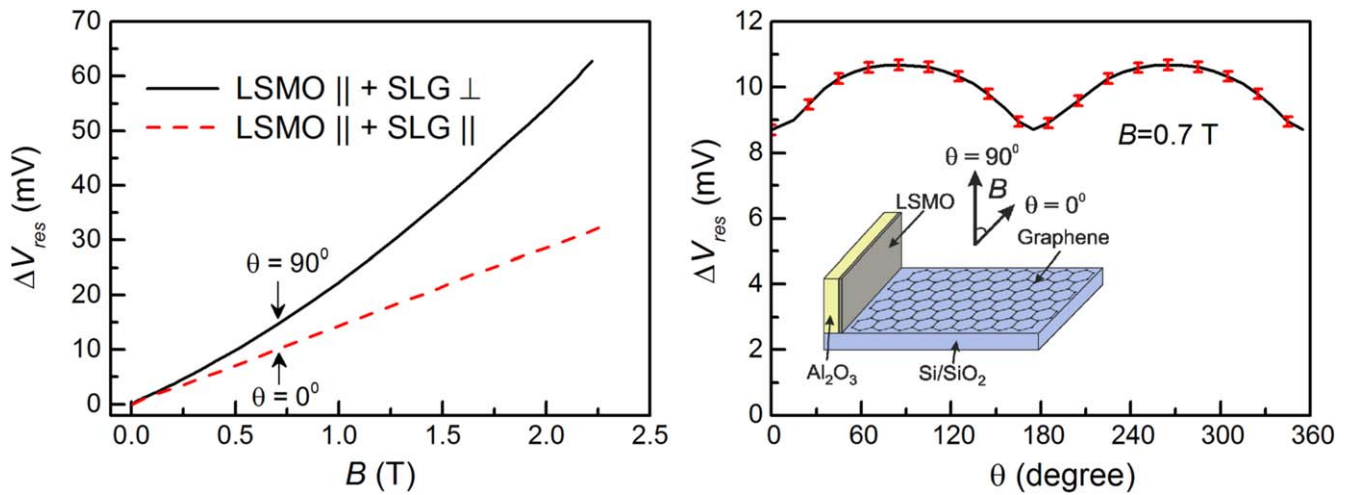


Figure 5. (a) The response ΔV_{res} versus B dependence of hybrid GM sensor at two magnetic field orientations. Solid black curve obtained when B was parallel to manganite film plane and perpendicular to graphene layer ($\theta = 90^\circ$, see inset in (b) graph). Dashed curve obtained when B was parallel to both manganite film and graphene planes ($\theta = 0^\circ$). (b) The response of hybrid GM sensor at different angles θ of 0.7 T magnetic field direction in respect to the graphene plane (shown in inset). $T = 294$ K.

manganite plane (red dashed curve) and (2) when B is parallel to manganite film plane and perpendicular to graphene layer plane (black solid curve). The difference between solid and dotted curves shows the influence of magnetoresistance effect of graphene layer (SLG magnetoresistance is zero for in-plane configuration) on total response of the sensor. Figure 5(b) also demonstrates how hybrid graphene-manganite sensor can be applied for position sensing. When B is parallel to graphene layer, the response of the sensor shows only magnetic field which is proportional to the distance to a permanent magnetic field source (response only from manganite sensor). In such case the GM sensor operates as proximity (position) sensor. After reaching the defined distance the object containing GM sensor can be rotated in respect to the permanent magnet and additional response signal (due to graphene layer) changing on the angle θ appears. In the latter case the GM sensor operates as an angle sensor. The curve presented in figure 5(b) shows the dependence of the total response of the hybrid GM sensor at 0.7 T on the angle of magnetic field in respect to graphene plane. One can evaluate the sensitivity of the sensor: the trace change with the rotation angle is (2 ± 0.07) mV at 0.7 T and it amounts approximately 22% of the basic signal (~ 9 mV). It is difficult to compare the sensitivity of such sensor with commercial GMR or AMR angle and position sensors operating at much lower magnetic fields (for example, relative sensitivity of 0.112 mV/VOe of GMR sensor was obtained in the range of ± 50 Oe [46]). Comparing to other sensors, the proposed GM sensor has advantages as it will be able to detect objects with larger tolerance for the air gap (not saturates at higher magnetic field and has wider operation range). Moreover, the use of one single sensor with position and angle sensing options instead of several sensors is an advantage in many applications.

4. Conclusions

In conclusion, we have demonstrated a novel magnetic field sensor based on hybrid structure of a SLG and thin nanostructured manganite film which a sense layer thickness depending on fabrication conditions and design configuration can be minimized to micro-nanoscale dimensions. The hybrid graphene-manganite sensor is designed in a Wheatstone half-bridge in which both sensing elements SLG and LSMO are connected in series, thus two effects of nanomaterials—large positive magnetoresistance of graphene and large negative magnetoresistance of nanostructured manganite film allowed us significantly increase the sensitivity of the hybrid GM sensor in comparison with individual SLG and LSMO sensors. Moreover, the hybrid graphene-manganite sensor has lower sensitivity to temperature variations in comparison to the manganite sensor and can be applied for position sensing.

Acknowledgments

RL acknowledge funding provided by the European Union and Marie Skłodowska-Curie Actions (2016–2017) Grant No. 751905. NZ and RN are grateful for the partial research funding by the European Regional Development Fund according to the supported activity ‘Research Projects Implemented by World-class Researcher Groups’ under Measure No. 01.2.2-LMT-K-718, Grant No. DOTSUT-235.

ORCID iDs

Rasuole Lukose <https://orcid.org/0000-0003-0154-2656>
 Nerija Zurauskiene <https://orcid.org/0000-0003-0912-4563>

References

- [1] Pisana S, Braganca P M, Marinero E E and Gurney B A 2010 *Nano Lett.* **10** 341
- [2] Deng Z, Yenilmez E, Leu J, Hoffman J E, Straver E W J, Dai H and Moler K A 2004 *Appl. Phys. Lett.* **85** 6263
- [3] Cobas E, Friedman A L, van't Erve O M J, Robinson J T and Jonker T B 2012 *Nano Lett.* **12** 3000
- [4] Huang L, Zhang Z, Li Z, Chen B, Ma X, Dong L and Peng L M 2015 *ACS Appl. Mater. Interfaces* **7** 9581
- [5] Nabaee V, Chandrawati R and Heidari H 2018 *Biosens. Bioelectron.* **103** 69
- [6] Liu X, Lam K H, Zhu K, Zheng C, Li X, Du Y, Liu C and Pong P W T 2016 *CoRR* arXiv:1611.00317
- [7] Markevicius V, Navikas D, Zilyis M, Andriukaitis D, Valinevicius A and Cepenas M 2016 *Sensors* **16** 78
- [8] Schulz W and Geis I 2015 *IET Intell. Transp. Syst.* **9** 626
- [9] Haas F, Zellekens P, Lepsa M, Rieger T, Grützmacher D, Lüth H and Schäpers T 2017 *Nano Lett.* **17** 128
- [10] Jogschies L, Klaas D, Kruppe R, Rittinger J, Taptimthong P, Wienecke A, Rissing L and Wurz M C 2015 *Sensors* **15** 28665
- [11] Israel C, Calderón M J and Mathur N D 2007 *Mater. Today* **10** 24
- [12] Lenz J and Edelstein A S 2006 *IEEE Sens. J* **6** 631
- [13] Zhu K, Liu X and Pong P W T 2015 *IEEE Transactions on Instrumentation and Measurement* **1**
- [14] Stankevicius T, Medisaukas L, Stankevicius V, Balevicius S, Zurauskiene N, Liebfried O and Schneider M 2014 *Rev. Sci. Instrum.* **85** 044704
- [15] Staruch M and Jain M J 2014 *Solid State Chem.* **214** 12
- [16] Balevicius S, Zurauskiene N, Stankevicius V, Kersulis S, Plausinaitiene V, Abrutis A, Zherlitsyn S, Herrmannsdorfer T, Wosnitza J and Wolff-Fabris F 2012 *Appl. Phys. Lett.* **101** 092407
- [17] Žurauskienė N, Balevičius S, Pavilionis D, Stankevič V, Plaušiniaitienė V, Zherlitsyn S, Herrmannsdörfer T, Law J M and Wosnitza J 2014 *IEEE Trans. Magn.* **50** 6100804
- [18] Haghiri-Gosnet A M and Renard J P 2003 *J. Phys. D: Appl. Phys.* **36** R127
- [19] Ziese M 2002 *Rep. Prog. Phys.* **65** 143
- [20] Zhang Z, Ranjith R, Xie B T, You L, Wong L M, Wang S J, Wang J L, Prellier W, Zhao Y G and Wu T 2010 *Appl. Phys. Lett.* **96** 222501
- [21] Li X W, Gupta A, Xiao G and Gong G Q 1997 *Appl. Phys. Lett.* **71** 1124
- [22] Yunhui X, Dworak V, Drechsler A and Hartmann U 1999 *Appl. Phys. Lett.* **74** 2513
- [23] Zurauskiene N, Balevicius S, Stankevicius V, Kersulis S, Schneider M, Liebfried O, Plausinaitiene V and Abrutis A 2011 *IEEE Trans. Plasma Sci.* **39** 411
- [24] Schneider M, Liebfried O, Stankevicius V, Balevicius S and Zurauskiene N 2009 *IEEE Trans. Magn.* **45** 430
- [25] Balevičius S, Žurauskienė N, Stankevič V, Herrmannsdörfer T, Zherlitsyn S, Skourski Y, Fabris F W and Wosnitza J 2013 *IEEE Trans. Magn.* **49** 5480
- [26] Novoselov K S, Geim A K, Morozov S V, Jiang D, Katsnelson M I, Grigorieva I V, Dubonos S V and Firsov A A 2005 *Nature* **438** 197
- [27] Gopinadhan K, Jun Shin Y, Jalil R, Venkatesan T, Geim A K, Castro Neto A H and Yang H 2015 *Nat. Commun.* **6** 8337
- [28] Kisslinger F, Ott C, Heide C, Kampert E, Butz B, Spiecker E, Shallcross S and Weber H B 2015 *Nat. Phys.* **11** 650
- [29] Friedman A L *et al* 2010 *Nano Lett.* **10** 3962
- [30] Liu Y, Liu X, Zhang Y, Xia Q and He J 2017 *Nanotechnology* **28** 235303
- [31] Dauber J, Sagade A A, Oellers M, Watanabe K, Taniguchi T, Neumaier D and Stampfer C 2015 *Appl. Phys. Lett.* **106** 193501
- [32] Rahman M W, Bodepudi C and Pramanik S 2018 *Nanotechnology* **29** 385202
- [33] Orlita M, Escoffier W, Plochocka P, Raquet B and Zeitler U 2013 *C. R. Phys.* **14** 78
- [34] Zurauskiene N, Balevicius S, Stankevicius V, Kersulis S, Klimantavicius J, Plausinaitiene V, Kubilius V, Skapas M, Juskenas R and Navickas R 2018 *J. Mater. Sci.* **53** 12996
- [35] Mathews M, Postma F M, Lodder J C, Jansen R, Rijnders G and Blank D H A 2005 *Appl. Phys. Lett.* **87** 242507
- [36] Zurauskiene N, Kersulis S, Medisaukas L and Tolvaisiene S 2011 *Acta. Phys. Pol. A* **119** 186
- [37] Žurauskiene N, Pavilionis D, Klimantavicius J, Balevicius S, Stankevicius V, Vasiliauskas R, Plausinaitiene V, Abrutis A, Skapas M and Juškenas R 2017 *IEEE Trans. Plasma Sci.* **45** 2773
- [38] Evetts J E, Blamire M G, Mathur N D, Isaac S P, Teo B S, Cohen L F and Macmanus-Driscoll J L 1998 *Phil. Trans. R. Soc. A* **356** 1593
- [39] Silva A V, Leitao D, Valadeiro J, Amaral J, Freitas P P and Cardoso S 2015 *Eur. Phys. J. Appl. Phys.* **72** 10601
- [40] Dauber J, Sagade A A, Oellers M, Watanabe K and Taniguchi T 2015 *Appl. Phys. Lett.* **106** 193501
- [41] Lukose R *et al* 2019 *Beilstein J. Nanotechnol.* **10** 256
- [42] Liu Y *et al* 2018 *Nano Lett.* **18** 3377
- [43] Schneider M, Spahn E, Balevicius S, Zurauskiene N and Stankevicius V 2018 *EU Patent* 2 040 088 B1
- [44] Fleming A J 2013 *Sensors Actuators A* **190** 106
- [45] Hahn R, Langendorf S, Seifart K, Slatter R, Olberts B and Romera F 2016 *Proc. 43rd Aerospace mechanisms Symp.* pp 177–83
- [46] Yan S, Cao Z, Guo Z, Zheng Z, Cao A, Qi Y, Leng Q and Zhao W 2018 *Sensors* **18** 1832